BAYESIAN ANALYSIS FOR A NEW CLASS OF HYBRID EoS MODELS USING MASS AND RADIUS DATA OF COMPACT STARS*

A. Ayriyan[a], D.E. Alvarez-Castillo[b,c], S. Benic[d]
D. Blaschke[b,e,f], H. Grigorian[a,g], S. Typel[h,c]

[a]Laboratory of Information Technologies, JINR, Dubna, Russia
[b]Bogoliubov Laboratory for Theoretical Physics, JINR, Dubna, Russia
[c]GSI Helmholtzzentrum für Schwerionenforschung GmbH, Darmstadt, Germany
[d]Physics Department, University of Zagreb, Zagreb, Croatia
[e]Institute of Theoretical Physics, University of Wrocław, Wrocław, Poland
[f]National Research Nuclear University (MEPhI), Moscow, Russia
[g]Department of Theoretical Physics, Yerevan State University, Yerevan, Armenia
[h]Institut für Kernphysik, Technische Universität Darmstadt
Darmstadt, Germany

We present a Bayesian analysis for a new class of realistic models of two-phase equations of state (EoS) for hybrid stars and demonstrate that the observation of a pair of high-mass twin stars would have a sufficient discriminating power to favour hybrid EoS with a strong first-order phase transition over alternative EoS. Such a measurement would provide evidence for the existence of a critical endpoint in the QCD phase diagram.

1. Introduction

In this contribution, we present results of a Bayesian analysis (BA) performed with a new class of realistic models of two-phase equations of state (EoS) for hybrid stars that allows for a broad variety of mass-radius (M-R) sequences upon variation of two EoS parameters [1]. These include ordinary neutron stars, stable hybrid star branches connected to neutron star ones and branches disconnected from the neutron star ones. A disconnected hybrid star branch, also called "third family", covers also a mass range of high-mass twin stars [2, 3] characterized by the same gravitational mass but different radii. For the classification of M-R sequences with hybrid stars, see [4].

---

* Presented at the "Critical Point and Onset of Deconfinement" Conference, Wrocław, Poland, May 30–June 4, 2016.

The new class of two-phase EoS is characterized by three main features:

(1) stiffening of the nuclear EoS at supersaturation densities due to quark exchange effects (Pauli blocking) between hadrons, modelled by an excluded-volume correction,

(2) stiffening of the quark matter EoS at high densities due to multiquark interactions, and

(3) possibility for a strong first-order phase transition with an early onset and large density jump.

The third feature results from a Maxwell construction for the possible transition from the nuclear to the quark matter phase and its properties depend on the two parameters determining the properties (1) and (2), respectively. Varying these two parameters, one obtains a class of hybrid EoS that yields solutions of the Tolman–Oppenheimer–Volkoff (TOV) equations for sequences of hadronic and hybrid stars in the mass-radius diagram which cover the full range of patterns according to the Alford–Han–Prakash classification [4].

We will use the BA to demonstrate that the observation of a pair of high-mass twin stars would have a sufficient discriminating power to favour hybrid EoS with a strong first-order phase transition over alternative EoS [1].

2. New class of quark–hadron EoS for hybrid stars

In this study, hybrid neutron stars that are composed of hadronic matter might undergo a phase transition to quark matter in their cores if parameter values of the models physically allow for it.

For the hadronic part of the neutron star EoS, we consider here the density-dependent relativistic mean-field EoS named "DD2F−" which is slightly softer than "DD2" [5] as it fulfils the flow constraint from heavy-ion collision experiments [6] and has a soft symmetry energy. The excluded-volume correction is applied to hadronic matter at suprasaturation densities and has the effect of stiffening the EoS without modifying any of the experimentally well-constrained properties below and around the saturation density $n_{\mathrm{sat}} = 0.16$ fm^{-3}. We introduce the available volume fraction Φ_N for the motion of nucleons at a given density n as [7]

$$\Phi_N = \left\{ \begin{array}{ll} 1\,, & \text{if} \quad n \leq n_{\mathrm{sat}}\,, \\ \exp\left[-v|v|(n - n_{\mathrm{sat}})^2/2\right]\,, & \text{if} \quad n > n_{\mathrm{sat}}\,, \end{array} \right.$$

with $v = 16\pi r_N^3/3$ as the van der Waals excluded volume corresponding to a nucleon hard-core radius r_N. In this work, the dimensionless parameter $p = 10 \times v\,[\mathrm{fm}^3]$ is introduced, taking values $p = 0, 5, 10, \ldots, 80$.

The quark matter EoS models in the high-density phase are obtained from an NJL model with multiquark interactions [2, 8] where the thermodynamic potential for two quark flavours, $q = (u, d)$, within the mean-field approximation is

$$\Omega = U + \sum_{f=u,d} \Omega_f \left(M_f, T, \tilde{\mu}_f \right) - \Omega_0 \,,$$

$$\Omega_f = -2N_c \int \frac{\mathrm{d}^3 p}{(2\pi)^3} \left\{ E_f + T \ln \left[1 + e^{-\beta(E_f - \tilde{\mu}_f)} \right] + T \ln \left[1 + e^{-\beta(E_f + \tilde{\mu}_f)} \right] \right\} \,,$$

$$U = \frac{2g_{20}}{\Lambda^2} \left[\left(\phi_u^2 + \phi_d^2 \right) - \eta_2 \left(\omega_u^2 + \omega_d^2 \right) \right] + \frac{12g_{40}}{\Lambda^8} \left[\left(\phi_u^2 + \phi_d^2 \right)^2 - \eta_4 \left(\omega_u^2 + \omega_d^2 \right)^2 \right] \,.$$

We neglected the mixing term $g_{22} = 0$ [8] and set $\eta_2 = 0.08$. The parameter η_4 is the dimensionless scaled coupling strength for the 8-quark interaction in the vector meson channel which determines the stiffness of the quark matter EoS at high densities. It will be varied in this study as $\eta_4 = 0, 1, 2, \ldots, 30$.
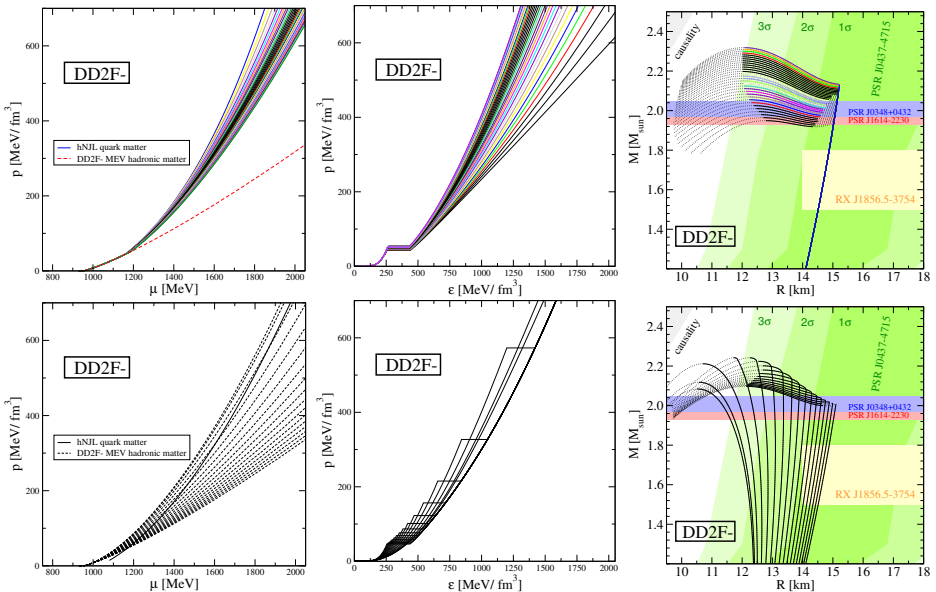

Fig. 1. (Colour on-line) Variations of the hybrid EoS for the DD2F− model for the fixed hadronic EoS (upper panels) and the fixed quark EoS (lower panels). The EoS is shown in the left and middle panels, the M-R diagrams in the right ones.

The phase transition in the hybrid EoS models is obtained by a Maxwell construction and therefore of first order. Having defined the hybrid EoS by a pair of parameters (p, η_4), the Tolman–Oppenheimer–Volkoff (TOV)

equations can be solved in a standard way resulting in a sequence of stars in the M-R diagram for each parameter set. A systematic analysis is performed by varying the EoS parameters, see Fig. 1.

3. Bayesian analysis for compact stars

BA is considered a powerful technique for model and parameter discrimination. The different observables taken into account for the present BA are the highest precisely measured masses $M_A = 2.01 \ M_\odot$ for PSR J0348+0432 [9] and $M_D = 1.94 \ M_\odot$ for PSR J1614-2230 [10, 11] with an error band $\Delta M_A = \Delta M_D = \pm 0.04 \ M_\odot$ as well as the radius determination $R_B = 15.5$ km with $\sigma_{R_B} = 1.5$ km by Bogdanov [12] for the nearest millisecond pulsar PSR J0437$-$4715. These constraints are shown by the coloured bands in the right panels of Fig. 1. They were already included in our earlier BA works [1, 13–16] where more details can be found.

In order to provide guidance for strategies of future observational programmes, we employ fictitious radius measurements. We assume that the radii R_A and R_D of both above-mentioned high-mass pulsars could be measured with a resolution characterized by the statistical uncertainty σ_{R_A} and σ_{R_D}, respectively.
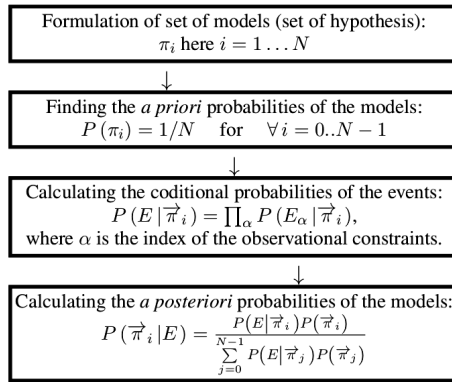

Fig. 2. The scheme of the Bayesian analysis technique for the EoS model using astrophysical data.

The vector of free parameters which correspond to all the possible models with or without nuclear to quark matter phase transition is defined as $\vec{\pi}_i = \{p_{(k)}, \eta_{4(l)}\}$, where $i = 0 \ldots N-1$ with $N = N_1 \times N_2$ such that $i = N_2 \times k + l$ and $k = 0 \ldots N_1 - 1$, $l = 0 \ldots N_2 - 1$, with N_1 and N_2 being the total number of parameters $p_{(k)}$ and $\eta_{4(l)}$, respectively. After integration of the TOV equations, each EoS model results in a curve in the M-R diagram for which the probability can be determined that this EoS fulfils the chosen

observational constraints. To this end, the conditional probabilities of these constraints are calculated which quantify how probable the observational data are for the assumed EoS model. The goal of the BA is to find the set of most probable $\vec{\pi}_i$ matching the above constraints using the BA technique (see Fig. 2).

4. Results and conclusions

In the left panel of Fig. 3, we show the BA results when using the mass constraint M_A together with the radius constraint R_B. One can see that the existing mass-radius constraints have a high selective power for the hadronic part of the considered EoS models, whereas for the quark phase they have practically no influence on the multiquark interaction parameter. The most probable values of the excluded-volume parameter is located in the ranges of $40 < p < 80$ in the two-dimensional parameter space (see Fig. 3).
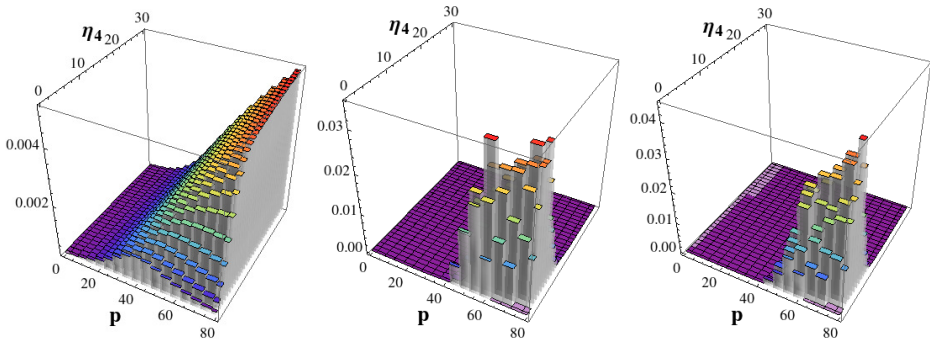

Fig. 3. BA of the probabilities in the EoS model parameter space $\eta_4 - p$ for separate mass and radius observation (M_A, R_B) (left panel) compared to fictitious radius measurements for known high-mass pulsars as high-mass twins with $(M_A, 13 \text{ km})$ and $(M_D, 15 \text{ km})$ for $\sigma_R = 1.5$ km (middle panel) and $\sigma_R = 0.5$ km (right panel).

Next, we have performed a BA assuming a set of fictitious radii (R_A, R_D) = (13 km, 15 km) for the known masses of the two high-mass pulsars. In the middle and right panels of Fig. 3, we present the results for the radius uncertainties of 1.5 km and 500 m, respectively. The results demonstrate that the simultaneous measurement of radii and masses of a pair of high-mass twin stars (here by assuming the possible outcome of radius measurements) could be strongly selective and could have sufficient discriminating power to favour hybrid EoS with a strong first-order phase transition over alternative EoS.

The next two steps in the development of the approach are devoted to an improvement of the variability of the dense-matter EoS within a two-dimensional parameter space embodying, *e.g.*, also the purely hadronic case without a phase transition and to mimic the occurrence of structures (so-called "pasta phases") in the phase transition region [17, 18].

REFERENCES

[1] D. Alvarez-Castillo *et al.*, *Eur. Phys. J. A* **52**, 69 (2016).

[2] S. Benić, *et al.*, *Astron. Astrophys.* **577**, A40 (2015).

[3] D. Alvarez-Castillo *et al.*, *Eur. Phys. J. A* **52**, 232 (2016).

[4] M.G. Alford, S. Han, M. Prakash, *Phys. Rev. D* **88**, 083013 (2013).

[5] S. Typel *et al.*, *Phys. Rev. C* **81**, 015803 (2010).

[6] P. Danielewicz, R. Lacey, W.G. Lynch, *Science* **298**, 1592 (2002).

[7] S. Typel, *Eur. Phys. J. A* **52**, 16 (2016).

[8] S. Benić, *Eur. Phys. J. A* **50**, 111 (2014).

[9] J. Antoniadis *et al.*, *Science* **340**, 6131 (2013).

[10] P. Demorest *et al.*, *Nature* **467**, 1081 (2010).

[11] E. Fonseca *et al.*, *Astrophys. J.* **832**, 167 (2016) [arXiv:1603.00545 [astro-ph.HE]].

[12] S. Bogdanov, *Astrophys. J.* **762**, 96 (2013).

[13] D.B. Blaschke *et al.*, *J. Phys.: Conf. Ser.* **496**, 012002 (2014).

[14] A. Ayriyan *et al.*, *Phys. Part. Nucl.* **46**, 854 (2015).

[15] D.E. Alvarez-Castillo *et al.*, eConf C140926 (2015) [arXiv:1506.07755 [astro-ph.HE]].

[16] A. Ayriyan *et al.*, *J. Phys.: Conf. Ser.* **668**, 012038 (2016).

[17] N. Yasutake *et al.*, *Phys. Rev. C* **89**, 065803 (2014).

[18] D.E. Alvarez-Castillo, D. Blaschke, *Phys. Part. Nucl.* **46**, 846 (2015).